International Journal of Modern Physics and Application
2015; 2(3): 19-27

ISSN: 2375-3870

American Association for Science and Technology

Keywords
Raman Spectra,
Raman Scattering Cross Sections,
Anisotropy Parameters,
Raman Polarizabilities and Phase Differences,
Nonlinear Least Square,
Relative Raman Tensor

Received: March 26, 2015
Revised: May 22, 2015
Accepted: May 23, 2015

A Simple Approach to Extract Some Optical Properties of Uniaxial Crystals from the Raman Spectrum: Case of Lithium Iodate ($LiIO_3$)

N. Djiedeu[1, *], B. Mohamadou[1], R. M. Erasmus[2], P. Bourson[3, 4], M. Aillerie[3, 4]

[1]Centre for Atomic Molecular Physics and Quantum Optics (CEPAMOQ), University of Douala, Douala, Cameroon
[2]School of Physics, University of the Witwatersrand, Johannesburg, South Africa
[3]Laboratoire Matériaux Optiques, Photonique et Systèmes (LMOPS)-EA 4423, Université de Lorraine, Metz, France
[4]Laboratoire Matériaux Optiques, Photonique et Systèmes (LMOPS), CentraleSupelec, Metz, France

Email address
djienico@yahoo.fr (N. Djiedeu), ballo_mohamadou@yahoo.fr (B. Mohamadou), Rudolph.Erasmus@wits.ac.za (R. M. Erasmus), bourson@metz.supelec.fr (P. Bourson), aillerie@metz.supelec.fr (M. Aillerie)

Citation
N. Djiedeu, B. Mohamadou, R. M. Erasmus, P. Bourson, M. Aillerie. A Simple Approach to Extract Some Optical Properties of Uniaxial Crystals from the Raman Spectrum: Case of Lithium Iodate ($LiIO_3$). *International Journal of Modern Physics and Application.*
Vol. 2, No. 3, 2015, pp. 19-27.

Abstract
In this work the improvement of the crystal rotation method established earlier for the quantitative analysis of the Raman spectra is presented. The integrated area is now a function of the damping parameter of the phonon modes, the phonon frequency and the maximum amplitude of the Lorentz profile. The cross sections are expressed as functions of the crystal rotation angle and the Raman polarizabilities through the anisotropy parameter. The integrated areas are fitted with a Lorentzian profile and evaluated. These areas are considered as experimental points for different crystal rotation angles to determine the angular dependence of the Raman scattering cross sections. A new nonlinear least square method (NLLSM) is used to derive the anisotropy parameters of the Raman polarizabilities and the cross sections for Transverse Optics (TO) modes. The derived quantities are later used to deduce the relative tensor of the Raman scattering cross sections. The phase differences of the Raman polarizabilities are deduced and therefore, the relative tensor of the Raman polarizabilities for the modes of the A symmetry. The angular dependence of the theoretical cross sections is also calculated for the modes of the E_1 and E_2 symmetries. The improvement of the crystal rotation method for the quantitative analysis of the Raman spectra is simple and leads to satisfactory results.

1. Introduction

Raman polarizabilities are important for the determination of electro-optic coefficients of materials. Despite proposals for absolute measurements by some authors [1], these coefficients have been given as approximations. Relative quantities obtained from a spectrometer are comparable to those obtained from other spectrometers so relative methods are currently preferred.

In the past decades, concerted efforts have been devoted to determine the Raman polarizabilities. Nippus [2], using a simplified Raman profile, established that the relative peak area is equivalent to the square of the relative Raman polarizabilitiesfor $LiNbO_3$. This model was not suitable because the proportionality coefficient depends on the phonon frequency. Kaminow and Johnston [3] have determined the absolute Raman scattering efficiencies of $LiNbO_3$ and $LiTaO_3$, but the results were incomplete due to some missing polarizability values. Johnston [4] using a theoretical approach determined the Raman polarizabilities with a sign uncertainty. Otaguro et al [5] using a relative method determined the second harmonic-generation coefficients and the linear electro-optic coefficient in $LiIO_3$ through oblique Raman measurements. Only one component of the Raman polarizability was extracted using this approach. More recently, Djiedeu *et al* [6] have calculated the anisotropy factors and the phase differences of the Raman polarizabilities for uniaxial crystals using the crystal rotation method based on the fit parameter reduction method (FPRM) which consists of reducing the number of variables in the cross section before the fitting operation.

The purpose of this work is the determination of the relative tensor of the Raman scattering cross sections and the relative tensor of the Raman polarizabilities in Lithium Iodate ($LiIO_3$) single crystal. The Lithium Iodate has interesting optical properties [7] and ionic conductivity character [8]. Section 2 presents an improvement of the integrated area evaluation and the general expression of the Raman cross section. In section 3, using the Raman polarizability tensors associated with the studied crystal point group, the cross sections are then expressed explicitly as functions of the crystal rotation angle and the anisotropy parameter. A new nonlinear least square method (NLLSM) associated with the FPRM is presented and used for the theoretical calculation of the cross sections. The residue is derived as a function of the anisotropy parameter which has a minimum for a unique value of the anisotropy parameter. The theoretical expressions for the relative tensor of the Raman scattering cross sections and the relative tensor of the Raman polarizabilities are then given. Section 4 presents the experimental and numerical results of the cross sections for some crystal rotation angles. The cross sections and the anisotropy parameters have been computed from the data using the Fortran 90 code and the relative values deduced. The phase differences of the Raman polarizabilities are also evaluated numerically. The generalization and the coherence of our method are then emphasized.

2. General Theory

2.1. Equivalence Between the Integrated Area and the Raman Scattering Cross Section

In general, the area A under a peak is defined by the expression

$$A = \int_b^c f(x)dx \tag{1}$$

The differential cross section has been predicted to have a Lorentzian profile [9]. Thus, if *f(x)* is the differential cross section, the integral will be the cross section that is the area under the peak. Nippus admitted this equivalence without an explicit demonstration [2]. We are going to determine the rough cross sections (cross section with arbitrary units) before deducing the relative cross sections.

The Raman intensity of a symmetric Raman line for a Transverse Optic (TO) mode can be written as follows [6]:

$$\frac{d^2I}{Id\omega d\Omega} = A_0 \frac{\Gamma\omega\omega_0^2}{\left(\omega^2-\omega_0^2\right)^2+\Gamma^2\omega^2}\left(n(\omega)+1\right) \tag{2}$$

A_0 is the amplitude of the Lorentzian profile and is now a dimensional quantity and not a pure constant. I is the ratio of the scattered and the incident light intensities. It is a dimensionless quantity. Ω: solid angle, ω_0: the phonon frequency, Γ: damping parameter of the phonon modes, $n(\omega)$: population factor. Dimensional analysis of Eq. (2) leads to $[A_0]=[\Omega]^{-1}=sr^{-1}$. Then A_0 has the inverse unit of a solid angle. The Raman intensity defined by Eq. (2) also has the inverse unit of a solid angle given that the remaining part of the Lorentzian profile is dimensionless.

The integrated areas obtained earlier [6] from Eq. (2) were independent of the damping parameter because of the approximation that was done, but the damping parameter was used to normalize those areas. Therefore, to improve the evaluation of these integrated areas, an approximation is made here only for the population factor, which doesn't change much from $\omega\sim\omega_0$. Using a change of variable, the integration of Eq. (2) in the interval $[0;+\infty]$, leads to:

$$S = \frac{dI}{Id\Omega} = \frac{1}{2}\Gamma S_{\max}\frac{\omega_0}{\sqrt{\omega_0^2-\Gamma^2/4}}\int_{z(0)}^{+\infty}\frac{1}{z^2+1}dz = \frac{1}{2}\Gamma S_{\max}\frac{\omega_0}{\sqrt{\omega_0^2-\Gamma^2/4}}\left[\frac{\pi}{2}+\arctan\left(\frac{\omega_0^2-\frac{\Gamma^2}{2}}{\Gamma\sqrt{\omega_0^2-\Gamma^2/4}}\right)\right] \tag{3}$$

Where

$$S_{\max} = A_0\frac{\omega_0}{\Gamma}\left(n(\omega_0)+1\right) \tag{4}$$

and

$$z(\omega) = \frac{\omega^2-\left(\omega_0^2-\frac{\Gamma^2}{2}\right)}{\Gamma\sqrt{\omega_0^2-\Gamma^2/4}}$$

S is the integrated area and $S_{\max}$ the height of the Lorentzian profile. $z(\omega)$ is the variable used for the integration. Eq. (3)

explicitly defines the Raman scattering cross section which equals the integrated area. The Raman scattering cross section now depends on the three main parameters of the Lorentz profile ($S_{\max}$, Γ, ω_0). For small values of the damping parameter, we retrieve the result published recently [6]. The only difference is that the variables used here are dimensional quantities.

Dimensional analysis of Eq. (3) shows that S has the unit of a cross section.

$$[S]=[S_{\max}][\Gamma]=[A_0][\Gamma]=sr^{-1}cm^{-1} \tag{5}$$

Instead of $sr^{-1}cm^{-1}$, arbitrary unit (a.u) will be used because $S_{\max}$ is generally given with arbitrary units.

2.2. Raman cross Section as Function of the Crystal Rotation Angle

The Raman scattering cross section of the optical mode is defined by [10,11,12]:

$$S_{\alpha\beta k}=\frac{dI_{s\alpha k}}{I_{i\beta}ld\Omega}=\sigma_{k,TO}{a_{\alpha\beta,k}}^2=\sigma_{k,TO}\left|\vec{e}_{s\alpha}^{\,*}P_k\vec{e}_{i\beta}\right|^2 \tag{6}$$

Where

$a_{\alpha\beta,k}$ is the Raman polarizability,

$$\sigma_{k,TO}=\frac{\hbar\left(\omega_i-\omega_k\right)^4\left(n_k+1\right)}{32\pi^2\varepsilon_0^2c^4\omega_k} \tag{7}$$

P_k is the Raman tensor. Instead of P_k we can also use:

$$P_k(\theta)=MP_kM^{-1} \tag{8}$$

$P_k(\theta)$ is the Raman tensor due to the rotation of the crystal and M is its rotation matrix because a θ rotation of the crystal corresponds to a $-\theta$ rotation of the polarization unit vectors [6].

α and β are the initial polar directions of the polarization unit vectors.

A relation similar to Eq. (8) was derived by Koningstein [13].

Using Eq.(6) and Eq. (8) we obtained:

$$S_{\alpha\beta k}=\sigma_{k,TO}\left|\vec{e}_{s\alpha}^{\,*}P_k(\theta)\vec{e}_{i\beta}\right|^2 \tag{9}$$

Eq. (3) is used to evaluate the Raman Scattering intensity from the experimental data and Eq. (9) is used to fit these points because they depend on the crystal rotation angle.

3. Crystal of C_6^6 Point Group: Case of the Lithium Iodate Crystal

The Lithium Iodate crystal belongs to the C_6^6 point group and the Raman polarizability tensors of the active modes are given by [14]:

$$A(z)=\begin{pmatrix}a&0&0\\0&a&0\\0&0&b\end{pmatrix},E_1(x)=\begin{pmatrix}0&0&c\\0&0&d\\c&d&0\end{pmatrix},E_1(y)=\begin{pmatrix}0&0&-d\\0&0&c\\-d&c&0\end{pmatrix}$$

$$E_2=\begin{pmatrix}e&f&0\\f&-e&0\\0&0&0\end{pmatrix},E_2=\begin{pmatrix}f&-e&0\\-e&-f&0\\0&0&0\end{pmatrix} \tag{10}$$

The letters in the parentheses (x,y,z) indicate the electric polarizations associated with the modes and the basic functions of the infra-red actives modes. The modes of the E_2 irreducible representations are Raman active and infra-red inactive. The theory of the crystal rotation [6] allows us to express the Raman scattering cross section as a function of the crystal rotation angle.

3.1. Rotation around the X Axis: Case of A Modes

We recall the Raman cross sections obtained recently [6] from Eq. (9) and Eq. (10) for A modes using the method of the crystal rotation. We can write these equations as the following forms:

$$S_{yz}^{A(\theta)}=S_{zy}^{A(\theta)}=(1/2)S_{ab}\left(1-\sin(2\beta)\cos\varphi_{ba}\right)\sin^2(2\theta) \tag{11}$$

$$S_{yy}^{A(\theta)}=S_{ab}\left(\cos^2\beta\cos^4\theta+\sin^2\beta\sin^4\theta+(1/4)\sin(2\beta)\cos\varphi_{ba}\sin^2(2\theta)\right) \tag{12}$$

$$S_{zz}^{A(\theta)}=S_{ab}\left(\cos^2\beta\sin^4\theta+\sin^2\beta\cos^4\theta+(1/4)\sin(2\beta)\cos\varphi_{ba}\sin^2(2\theta)\right) \tag{13}$$

Where the anisotropy parameter β is given by:

$$\cos\beta=\frac{|a|}{\sqrt{|a|^2+|b|^2}},\quad \sin\beta=\frac{|b|}{\sqrt{|a|^2+|b|^2}} \tag{14}$$

Let

$$r=\left(\sigma_{TO}\right)^{1/2}\left(|a|+i|b|\right)=|r|e^{i\beta} \tag{15}$$

$$S_r = r^2 = S_{ab}e^{2i\beta} \tag{16}$$

$$S_{ab} = |r|^2 = S_a + S_b = S_a\left(1+\tan^2\beta\right) \tag{17}$$

$$S_a = S_{ab}\cos^2\beta \tag{18}$$

$$S_b = S_{ab}\sin^2\beta \tag{19}$$

The magnitude of a complex number and its phase are independent variables. Hence, |r| and defined in Eq. (15) form a set of twoindependent variables. According to Eq. (16), Sab and are also independent variables.

Sa is the cross section associated with the a component of the Raman polarizability tensor. Sa can be measured experimentally and Sb deduced using Eq. (18) and Eq. (19). This was done earlier using the manual fitting (MF) and the fit parameter reduction method (FPRM) [6]. It is, however, not a systematic method because the two remaining variables are determined by manually fixing one and fitting the second. Here we propose to determine these parameters using a nonlinear least square method (NLLSM) associated with the FPRM. The cases of E1 mode and E2 mode are given in appendixes A and B.

3.2. Nonlinear Least Square Method Associated with the Fit Parameter Reduction Method: Case of A Modes

We combine the FPRM with the NLLSM adapted to these particular nonlinear equations for the area fitting procedure. It is a systematic method to evaluate the cross sections and the anisotropy parameter.

For A modes, Eq. (12) is used to determine the cross section tensor elements, the anisotropy parameter and the phase difference. Written in a polynomial form, Eq. (12) simplifies to:

$$S_{yy}^{A(\theta)} = S_{ab}\frac{1}{4}\left(\left(1-\sin 2\beta\cos\varphi_{ba}\right)\cos^2(2\theta)+2\cos 2\beta\cos(2\theta)+1+\sin 2\beta\cos\varphi_{ba}\right) = S_{ab}S(\beta,\theta) \tag{20}$$

The residue is thus given by the expression:

$$R = \sum_i \left(S_{ab}S(\beta,\theta_i)-S_i\right)^2 \tag{21}$$

where S_i is the cross section measured at each θ_i.

This residue has a global minimum value for the variation of S_{ab} and β.

The expression for S_{ab} is obtained by equating to zero the partial derivative of the residue with respect to S_{ab}. Hence we obtain:

$$S_{ab} = \frac{\sum_i S_i S(\beta,\theta_i)}{\sum_i S^2(\beta,\theta_i)} \tag{22}$$

By expanding the residue Eq. (21) as a second order polynomial equation and substituting S_{ab} (Eq. 22) in Eq. (21), the minimum of the residue due to the variation of S_{ab} is then given by:

$$R(\beta) = \sum_i S_i^2 - \frac{\left(\sum_i S_i S(\beta,\theta_i)\right)^2}{\sum_i S^2(\beta,\theta_i)} \tag{23}$$

$S(\beta,\theta_i)$ is obtained as a function of β only by replacing $\cos\varphi_{ba}$ by its expression ($p.\cos 2\beta$) obtained earlier [6] using the FPRM with p equal to plus or minus one. Using the experimental values of the cross section evaluated at each point θ_t, the quantities Eq. (22) and Eq. (23) have been calculated using a FORTRAN 90 code and the residue Eq. (23) plotted as a function of the anisotropy parameter. The curve has a minimum point. The abscissa of the minimum is the value of the anisotropy parameter. We succeed in extracting this anisotropy parameter using our code. Following, S_{ab} can be obtained by substituting this anisotropy parameter in Eq. (22) while S_a and S_b can then be deduced using Eq. (18) and Eq. (19). The numerical determination of the cross section and the anisotropy parameter for E modes can be deduced easily from the above results on A modes.

3.3. Relative Evaluation of the Raman Polarizabilities and the Raman Scattering Cross Sections

The relative quantities for the different modes have been deduced by dividing the results obtained from the previous calculations by some chosen quantities.

For A modes, a and S_a were used respectively for the Raman polarizabilities and the cross sections.

The relative tensor of the Raman polarizabilities (RP) is then given by:

$$RP(A(z)) = \begin{pmatrix} 1 & 0 & 0 \\ 0 & 1 & 0 \\ 0 & 0 & \frac{|b|}{|a|}e^{i\varphi_{ba}} \end{pmatrix} \tag{24}$$

$$\frac{|b|}{|a|} = tan\beta \tag{25}$$

The relative tensor of the Raman scattering cross sections (RCS) is then given by:

$$RCS(A(z)) = \begin{pmatrix} 1 & 0 & 0 \\ 0 & 1 & 0 \\ 0 & 0 & S_b/S_a \end{pmatrix} \tag{26}$$

$$\frac{S_b}{S_a} = tan^2\beta \tag{27}$$

We can see that relative quantities are functions of the anisotropy parameter β since φ_{ba} also depends on β [6]. This means that the anisotropy parameter is a very important quantity. We remind that the magnitude of the relative Raman polarizability (tangent of the anisotropy parameter) defined in Eq.(25) is also called the anisotropy factor [6].

4. Experiment and Numerical Results

In this part, we present the Raman spectrum for the geometrical configuration in used and the results of the numerical determination of the anisotropy parameters, the rough and relative cross sections, the relative Raman polarizabilities and their phase differences.

4.1. Raman Spectra of a Pure LiIO$_3$

The experiments were done at a temperature of 296K with the integration time of 30s. The laser power at the sample was 1.30mW. This was measured using a Coherent Field Master GS power meter with model LM-2 power sensor. The 514.5nm line of an argon ion laser and a Jobin Yvon T64000 Raman spectrometer operated in triple subtractive mode was used to collect these spectra. The samples were polished on the two faces perpendicular to the x direction.The spectra are measured with 10° rotation step intervals around the x axis, thus in the yz plane. The recorded spectra are reported in Fig. 1 in backscattering configuration x(yy)x.

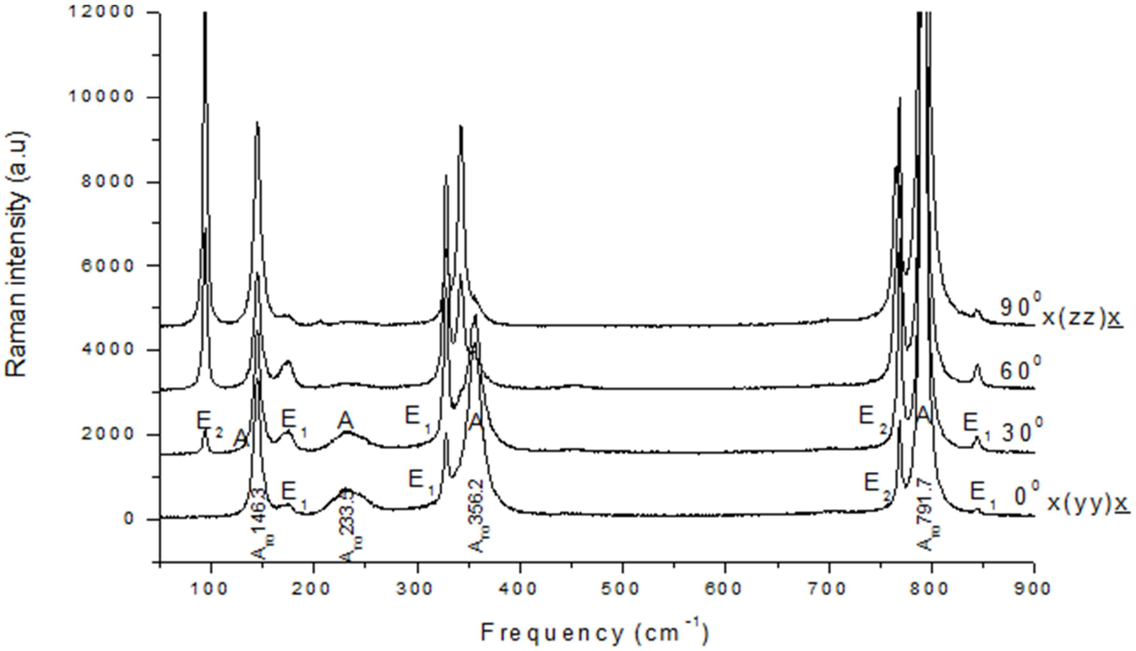

Fig. 1. Raman spectra of a pure LiIO$_3$; rotation around the x axis (yz plane).

The 4 frequencies of A modes have been observed in these spectra and are in agreement with the literature [5,15,16]. Especially in [16], the temperature dependence of the Raman spectra for A modes of the α-LiIO$_3$ has been studied to point out the nature and role of the defects. When we consider the Raman responses from 0 to 90°, we observed the emergence of the peaks of E$_2$ mode at 95cm^{-1} and that of A mode at 791.7cm^{-1}. Simultaneously, the peak of A mode at 233.5cm^{-1}disappears.

4.2. Evaluation of the Integrated Areas

Table 1 displays the integrated areas obtained for the 4 vibrational modes of the A symmetry specie of the Lithium Iodate crystal for some crystal rotation angles.

***Table 1.** Integrated areas.*

Angle	ω_0 (cm^{-1})	A$_0$ (a.u)	Γ (cm^{-1})	S$_{max}$(a.u)	S(a.u)
0	145.3	89.6	7.7	3337	32889
	233.5	64.4	33.6	659	28078
	356.2	161.0	16.8	4147	89229
	791.7	175.7	5.1	27811	182817
30	145.3	73.5	7.1	2952	26990
	233.5	46.9	31.5	512	20474
	356.2	116.9	15.4	3285	64827
	791.7	137.2	4.7	23664	142782
60	145.3	75.6	7.7	2816	27756
	233.5	21.0	43.4	167	9134
	356.2	39.9	18.9	913	22080
	791.7	163.8	5.0	26661	170458

Angle	ω_0 (cm^{-1})	A_0 (a.u)	Γ (cm^{-1})	S_{max}(a.u)	S(a.u)
90	145.3	129.5	7.7	4825	47555
	233.5	16.7	42.7	135	7260
	356.2	24.5	16.1	660	13603
	791.7	283.5	4.6	50403	295040

4.3. Anisotropy Parameter at the Minimum Point of the Residue and Numerical Results

Fig. 2 displays the variation of the residue as a function of the anisotropy parameter for 791.7cm^{-1} frequency. The anisotropy parameter can be found by considering the minimum point of the residue. With the use of a program written in Fortran 90, we have fitted the integrated areas listed in Table 1 to obtain the expected values of the cross sections defined in Eq.(20) and the residue defined in Eq. (23). The optical properties obtained as results of the fitting program, i.e. the anisotropy parameter β, the phase difference φ_{ba}, the relative cross section and the magnitude of the relative polarizability are listed in Table 2. The relative errors are also listed.

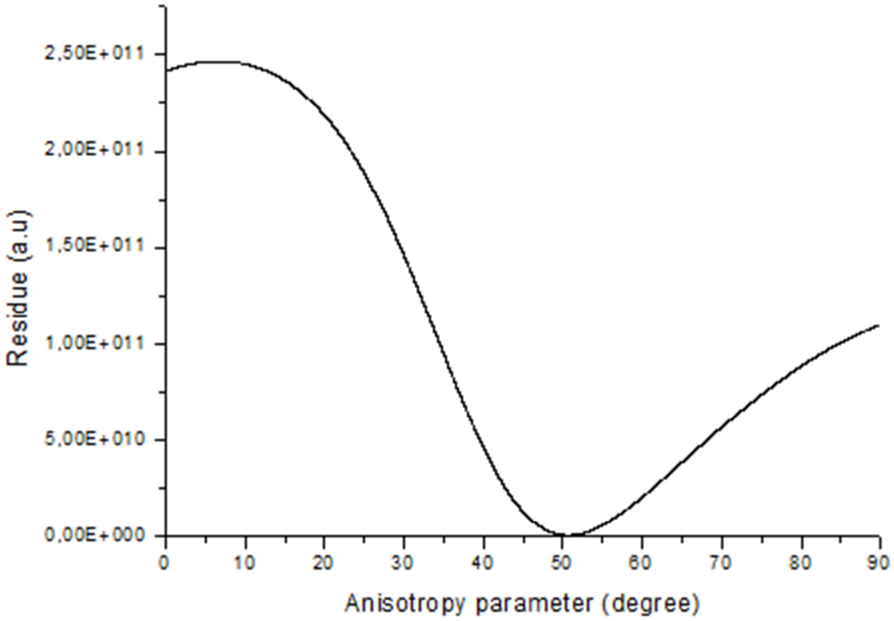

Fig. 2. *Variation of the residue as a function of the anisotropy parameter for the 791.7cm^{-1} line; rotation around the x axis (yz plane).*

Table 2. *Optical properties deduced from the fit.*

ω_0(cm^{-1})	S_{ab}(a.u)	S_a(a.u)	S_b(a.u)	β (deg)	φ_{ba}(deg)	R.C.S^c S_b/S_a	M.R.P^d $\vert b\vert/\vert a\vert$	R.Er^e (%)
145.3	79459	34723	44737	48.62	82.76	1.29	1.13	5.12
233.5	35706	28452	7254	26.79	53.58	0.25	0.50	3.05
356.2	104410	90707	13703	21.24	42.48	0.15	0.39	2.89
791.7	458546	184348	274198	50.65	78.70	1.49	1.22	4.69

[c]: relative cross section.
[d]: magnitude of the relative polarisability
[e]: relative error

Table 3. *Relative tensors of the Raman cross sections and the Raman polarizabilities.*

0 (cm-1)		233.5	356.2	791.7
RCS(A(z))	$\begin{matrix}1&0&0\\0&1&0\\0&0&1,29\end{matrix}$	$\begin{matrix}1&0&0\\0&1&0\\0&0&0.25\end{matrix}$	$\begin{matrix}1&0&0\\0&1&0\\0&0&0.15\end{matrix}$	$\begin{matrix}1&0&0\\0&1&0\\0&0&1.49\end{matrix}$
RP(A(z))	$\begin{matrix}1&0&0\\0&1&0\\0&0&1.13e^{82.76i}\end{matrix}$	$\begin{matrix}1&0&0\\0&1&0\\0&0&0.50e^{53.58i}\end{matrix}$	$\begin{matrix}1&0&0\\0&1&0\\0&0&0.39e^{42.48i}\end{matrix}$	$\begin{matrix}1&0&0\\0&1&0\\0&0&1.22e^{78.70i}\end{matrix}$

The rough cross sections evaluated above (S_{ab}, S_a, S_b) and obtained for a particular spectrometer cannot be compared directly to those obtained from other spectrometers because they are given with arbitrary units. Meanwhile, relative quantities (cf. Table 3) obtained with this method are comparable with those obtained from other spectrometers.

Figures 3 and 4 represent theoretical simulations and experimental data of the Raman scattering cross sections for A modes as functions of the crystal rotation angle evaluated respectively at 356.2cm^{-1} and 791.7cm^{-1}.

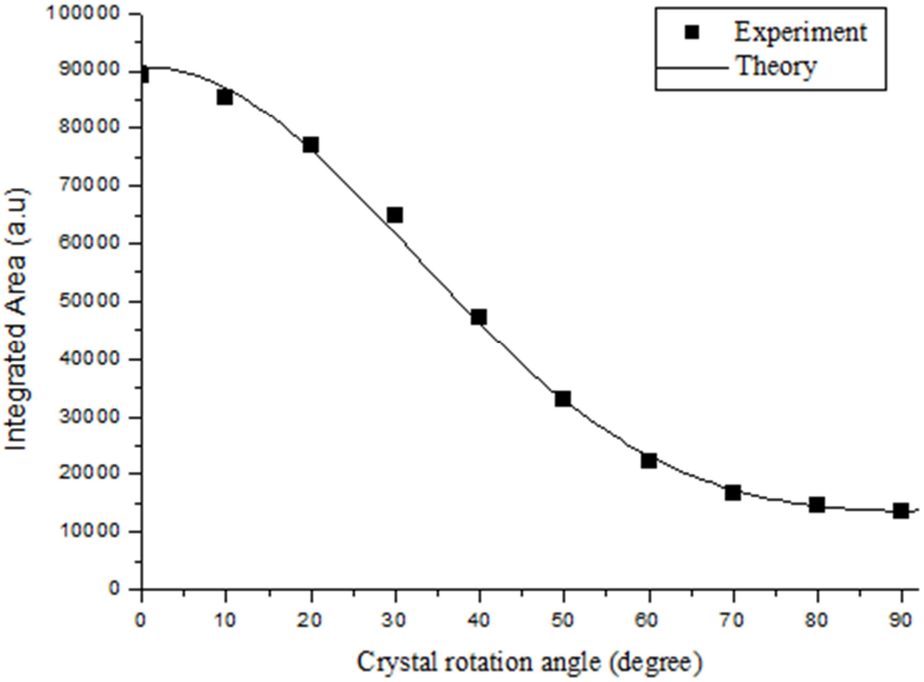

Fig. 3. *Theory and experiment at 356.2cm^{-1}; rotation around the x axis (yz plane).*

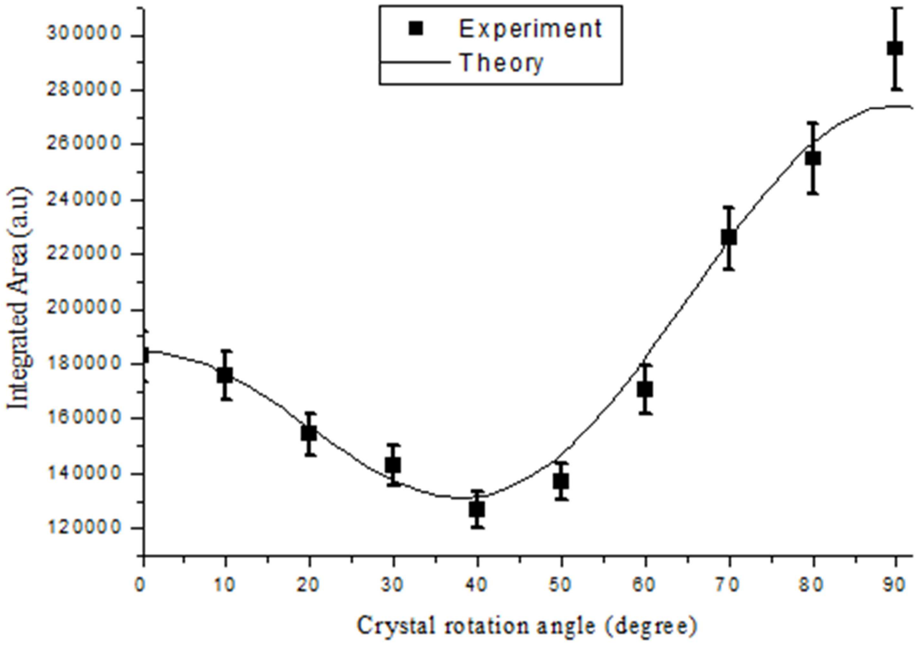

Fig. 4. *Theory and experiment at 791.7cm^{-1}; rotation around the x axis (yz plane).*

Figures 3 and 4 show that the NLLSM associated with the FPRM is in good agreement with the experiment. This method is preferable than the manual fitting (MF) associated with the FPRM presented earlier [6] because it allows the minimization of the residue. Especially in Fig. 4, we can note that the final experimental point 90° (for 791.7cm^{-1}) is not good because it increases the error and modifies slightly the profile of the curve. This may be due to the term containing the phase difference in the cross section which does not contribute at the extremalpoints (0 and 90°). Table 2 shows that the errors are less than 6%. In some previous studies on $LiNbO_3$ not all quantities were provided (Kaminow and Johnston [3]). In addition, in these studies, the cross sections and the Raman polarizabilities were determined with very large errors sometimes more than 50% (Johnston [4]). Useful comparison with previous work on $LiIO_3$ is difficult due to the nature of the relative method used.

5. Conclusion

In this work, a systematic method for the determination of the relative tensor of the Raman scattering cross sections, the relative tensor of the Raman polarizabilities is presented. The theory of the crystal rotation presented earlier has been improved. A new approach for the determination of the anisotropy parameter and the cross section using the nonlinear least square method associated with the fit parameter reduction method has been developed. It appears in this work that the anisotropy parameter is the most important parameter for the determination of some optical properties of crystals. This method is the appropriate approach for the theoretical analysis of the Raman scattering cross sections obtained from the theory of the crystal rotation on the one hand and the quantitative analysis of the integrated areas obtained from the Raman spectra on the other hand. This work can be extended to the determination of the longitudinal cross section. Other crystals can be investigated as well as other laser excitation wavelengths.

Acknowledgment

The authors would like to thank the African Laser Center (ALC) for the financial support of this work.

Thanks are also addressed to Dr D.Wamwangi for fruitful discussions of this work.

Appendixes

A. Rotation Around the Z Axis: Case of E_1 Modes

A rotation around the z axis allows us to express the Raman cross section for E_{1x} symmetry:

$$S_{xz}^{E_{1x}(\theta)} = S_{zx}^{E_{1x}(\theta)} = \frac{1}{2}S_{cd}\left(1+\cos(2\alpha)\cos(2\theta)+\sin(2\alpha)\cos\varphi_{dc}\sin(2\theta)\right) \tag{A.1}$$

$$S_{yz}^{E_{1x}(\theta)} = S_{zy}^{E_{1x}(\theta)} = \frac{1}{2}S_{cd}\left(1-\cos(2\alpha)\cos(2\theta)-\sin(2\alpha)\cos\varphi_{dc}\sin(2\theta)\right) \tag{A.2}$$

Where the anisotropy parameter α is given by:

$$\cos\alpha = \frac{|c|}{\sqrt{|c|^2+|d|^2}}, \quad \sin\alpha = \frac{|d|}{\sqrt{|c|^2+|d|^2}} \tag{A.3}$$

$$S_{cd} = \sigma_{TO}\left(|c|^2+|d|^2\right) = S_c + S_d = S_c\left(1+\tan^2\alpha\right) \tag{A.4}$$

$$S_c = S_{cd}\cos^2\alpha \tag{A.5}$$

$$S_d = S_{cd}\sin^2\alpha \tag{A.6}$$

The cross sections given by Eq. (A.1) and Eq. (A.2) are measurable for propagation directed along the y axis and the x axis respectively in the backscattering geometry. Finally, Eq. (A.1) and Eq. (A.2) allow the choice of the E_{1x} or E_{1y} symmetries.

B. Rotation Around the Z Axis: Case of E_2 Modes

For E_2 modes, the results are the following:

$$S_{xx}^{E_2(\theta)} = S_{yy}^{E_2(\theta)} = \frac{1}{2}S_{ef}\left(1+\cos(2\gamma)\cos(4\theta)-\sin(2\gamma)\cos\varphi_{fe}\sin(4\theta)\right) \tag{B.1}$$

$$S_{xy}^{E_2(\theta)} = S_{yx}^{E_2(\theta)} = \frac{1}{2}S_{ef}\left(1-\cos(2\gamma)\cos(4\theta)+\sin(2\gamma)\cos\varphi_{fe}\sin(4\theta)\right) \tag{B.2}$$

$$\cos\gamma = \frac{|e|}{\sqrt{|e|^2+|f|^2}}, \quad \sin\gamma = \frac{|f|}{\sqrt{|e|^2+|f|^2}} \tag{B.3}$$

$$S_{ef} = \sigma_{TO}\left(|e|^2+|f|^2\right) = S_e + S_f = S_e\left(1+\tan^2\gamma\right) \tag{B.4}$$

$$S_e = S_{ef}\cos^2\gamma \tag{B.5}$$

$$S_f = S_{ef}\sin^2\gamma \tag{B.6}$$

For the propagation along the z axis direction, the cross sections given by equation Eq. (B.1) and Eq. (B.2) are measurable in the backscattering geometry for parallel and perpendicular polarizations, respectively. Due to the presence of an ionic conductivity when an electric field propagates along the optical axis (z) of an $LiIO_3$ crystal, its optical properties are not of interest [17] for this case of propagation.

References

[1] P. Knoll and H. Kuzmany, Phys. Rev. B 29(1984)2221-6

[2] M. Nippus, Z.Naturforsch, a 31 (1976)231-5

[3] I.P. Kaminow, W.D. Johnston and Jr., Phys. Rev. 160(1967)519 and 178(Errata 1969)1528

[4] W.D. Johnston and Jr., Phys. Rev. B1(1970)3494

[5] W.S. Otaguro, E. Wiener-Avnear and S.P.S. Porto, Applied Phys. Letters 18(1971)499-501

[6] N. Djiedeu, B. Mohamadou, P. Bourson and M. Aillerie, J.Phys.: Condens. Matter 21(2009)015905

[7] C. Robert Eckardt, Member, IEEE, Hisashi Masuda, Yuan Xuan Fan, and Robert L. Byer, Fellow IEEE, J. of Quantum Electron. 26(1990)922-933

[8] Y. Mugnier, C. Galez, J.M. Crettez, P. Bourson and J. Bouillot, Solid State Commun 115(2000)619-623

[9] A.S. Barker, Jr. and R. Loudon, Rev. Mod. Phys. 44(1972)18

[10] I.P. Kaminow and E.H. Turner, Phys. Rev. B 5(1972)1564

[11] P. Knoll, H. Kuzmany, Phys. Rev. B 29(1984)2221

[12] N. Djiedeu, B. Mohamadou, P. Bourson and M. Aillerie, DOI 10.1051/names2007027 - http://names.edpsciences, 2008

[13] J.A. Koningstein, Introduction to Theory of the Raman Effect Copyright c by D. Reidel Publishing Company, Dordrecht, Holland,1972.

[14] W. Otaguro, E. Wiener-Avnear, C.A. Arguello and S.P.S. Porto, Phys.Rev.B4 (1971)4542-4551

[15] F.E.A. Melo and F. Cerdeira, Phys. Rev. B 26(1982)720

[16] Y. Mugnier, C. Galez, J.M. Crettez, P. Bourson, C. Opagiste and J. Bouillot, J.Solid State Chem 168(2002)76-84

[17] O.G. Vlokh, I.A. Velichko and L.A. Laz’ko, Sov. Phys. Crystallogr. 20(1975)263-4